14 Feb 2022

Effect of Interfacial Atomic Mixing on the Thermal Conductivity of Multi-Layered Stacking Structure

Yingguang Liu

Xinqiang Xue

Guoliang Ren

Aleksandr V. Chernatynskiy
Missouri University of Science and Technology, aleksandrc@mst.edu

Recommended Citation

Y. Liu et al., "Effect of Interfacial Atomic Mixing on the Thermal Conductivity of Multi-Layered Stacking Structure," *Journal of Applied Physics*, vol. 131, no. 6, article no. 064301, American Institute of Physics, Feb 2022.
The definitive version is available at https://doi.org/10.1063/5.0078669

Effect of interfacial atomic mixing on the thermal conductivity of multi-layered stacking structure

Cite as: J. Appl. Phys. **131**, 064301 (2022); https://doi.org/10.1063/5.0078669
Submitted: 15 November 2021 • Accepted: 28 January 2022 • Published Online: 10 February 2022

Yingguang Liu, Xinqiang Xue, Guoliang Ren, et al.

Journal of Applied Physics ARTICLE scitation.org/journal/jap

Effect of interfacial atomic mixing on the thermal conductivity of multi-layered stacking structure

Cite as: J. Appl. Phys. **131**, 064301 (2022); doi: 10.1063/5.0078669
Submitted: 15 November 2021 · Accepted: 28 January 2022 ·
Published Online: 10 February 2022

Yingguang Liu,[1,a)] Xinqiang Xue,[1] Guoliang Ren,[1] and Aleksandr Chernatynskiy[2]

AFFILIATIONS

[1]Department of Power Engineering, School of Energy and Power Engineering, North China Electric Power University, Baoding 071003, China
[2]Physics Department, Missouri University of Science and Technology, Rolla, Missouri 65409, USA

[a)]**Author to whom correspondence should be addressed:** yingguang266@126.com

ABSTRACT

Multi-layered stacking structures and atomic mixing interfaces were constructed. The effects of various factors on the thermal conductivity of different lattice structures were studied by non-equilibrium molecular dynamics simulations, including the number of atomic mixing layers, temperature, total length of the system, and period length. The results showed that the mixing of two and four layers of atoms can improve the thermal conductivities of the multi-layer structure with a small total length due to a phonon "bridge" mechanism. When the total length of the system is large, the thermal conductivity of the multi-layer structure with atomic mixing interfaces decreases significantly compared with that of the perfect interfaces. The interfacial atom mixing destroys the phonon coherent transport in the multi-layer structure and decreases the thermal conductivity to some extent. The thermal conductivity of the multi-layer structure with perfect interfaces is significantly affected by temperature, whereas the thermal conductivity of the multi-layer structures with atomic mixing is less sensitive to temperature.

I. INTRODUCTION

According to Moore's law, the number of transistors that can be placed on an integrated circuit doubles about every 18 months. Moreover, the resulting heat dissipation of electronic devices is a major factor affecting their performance and efficiency. It is vital to remove the heat from the core of the device to an external radiator as efficiently as possible.[1–4] Due to the high surface-to-volume ratio in nanoscale components and devices, the heat transport at solid–solid interfaces often dominates the overall thermal transfer performance.[5,6] Therefore, reducing the interfacial thermal resistance is an explicit way to improve the overall heat transfer efficiency of nanomaterials. Heat transfer across the solid–solid interfaces, characterized by the thermal boundary conductivity (TBC) which determines effective thermal conductivity (TC) of the nanomaterials, is mainly controlled by the interfacial phonon transmission.[7–11] Important factors that affect the phonon transmission and, therefore, the TBC are the crystallographic orientation of the interface, crystal imperfections, and acoustic impedance mismatch.[12,13]

To enhance the thermal transfer capability at an interface between two solids, many methods have been proposed. Among the most common methods are the addition of thin films and the incorporation of atomic mixing. Recent theoretical[5] and experimental[14] studies have proved that interfacial thermal conductance can be manipulated by coupling the two solids of the interface with thin films. The "bridge" mechanism emerged as an explanation for this enhancement: atoms in the film provide vibrational modes that allow the better matching between dissimilar materials and, thus, improving phonon transmission. Similarly, the atomic mass of the thin film was optimized for the maximum effects on heat conduction,[15–17] and it was found that a material consisting of a certain thickness and mass gradient can greatly promote the heat transfer between two different solids.

The introduction of atomic mixing at an interface has shown to be an equally promising method to improve the thermal transport of highly acoustically mismatched single interface. These molecular dynamics studies attributed the improvement to the increased inelastic phonon scattering at the interfaces.[18,19] For instance, Tian *et al.*[20] conducted calculations using Green's function and concluded that atomic mixing at the interface can enhance the phonon transmission and interfacial thermal conductance, which is attributed to

the softened acoustic impedance at the interface and this greatly promotes the transport of phonons with mid-range frequencies. Most recently, Jia *et al.*[21] showed that the phonon transmission and thermal conductance of periodic rectangular-shaped and triangular-shaped Si/Ge interfaces are both enhanced and tunable by atomic mixing at the Si/Ge interface. For the triangular-shaped interface, the thermal conductance can be enhanced maximally by 22.3% compared with the perfect interface. The increased thermal conductance is attributed to that the mixed central region having a larger overlap frequency zone that will establish new channels to help the phonons transmit through the interface that they were initially not allowed to cross.

An actual nanoscale nanometer electronic device is usually a stacked structure with multi-layered interfaces. Different from the single interface mentioned above, the phonon transport mechanisms in multi-layered interface systems are more complex. Not only is the thermal transport performance related to the shape of the interfaces or the atomic bonding modes, but it is also affected by the period thickness, total length, and temperature. For a typical multi-layer structure (MLS) with multiple layers as an example, Ravichandran *et al.*[22] used epitaxial-growth techniques to synthesize superlattice structures and investigated the influence of the period length on the thermal transport. The results show that when the total length remains unchanged, the TCs of the superlattices decrease first, have a minimum, and then increase with the increase in the period length. Luckyanova *et al.*[23] used atomistic Green's function simulations to measure the TCs of the GaAs/AlAs superlattice. Their results show that the TCs increased gradually and eventually saturated at room temperature; they attributed this phenomenon to a transition from ballistic to diffusive transport. Chakraborty *et al.*[24] investigated the effect of interfacial atomic mixing on the thermal conductivity of superlattices and random multi-layer structures by non-equilibrium molecular dynamics (NEMD) simulations. The results show that interface species mixing can facilitate phonon transport in varying degrees of both superlattices and random multi-layer structures in the transition of phonon transport modes due to the phonon "bridge" effect. They did not delve into the effect of atomic mixing layers on the thermal conductivity in multi-layer structure (MLS).

In the above research studies, a single interface is taken as the research object, and the interface atomic structure is changed to improve the interfacial thermal conductivity, although this may not be fully applicable in guiding the heat dissipation design of nano-electronic devices with multi-layered stacking, and it is not clear how the atomic mixing at interfaces affects the thermal transport in systems with multi-layered interfaces. To further clarify the phonon transport mechanism, in this paper, we, therefore, take Si/Ge multi-layer structures as the research object, and the NEMD method was used to simulate the effect of interfacial atomic mixing degree on the thermal conductivity of such systems. The phonon transport mechanisms of perfect interface multi-layer structures and atomic mixed multi-layer structures at different total lengths, different cycle lengths, and different temperatures are compared. Especially, we focus on the coherent and incoherent phonon transport mechanisms under different structures.

II. MOLECULAR DYNAMICS MODEL

In this work, the NEMD simulations were used to calculate the thermal conductivities of different models. Assume that the lattice constants of Si and Ge are the same. The lattice constant of both Si and Ge is $a = 5.4307 \times 10^{-10}$ m. First, an Si/Ge interfacial structure with atomic mixtures of different thicknesses was analyzed at different temperatures, and the lengths of the leads at each side were kept at both approximately 10 nm along the X direction. A fixed boundary condition was used in the X direction and periodic boundary conditions were imposed in the Y and Z directions. In the central region, a certain number of layers was selected and the Si and Ge atoms were randomly shuffled while keeping the number ratio at 1 [n atomic mixture layers as shown in Figs. 1(b) and 1(d)]. The transverse cross-sectional area was set to be $6UC \times 6UC$ (unit cell: the lattice constant of Si), which has proved to be acceptable for TC calculations.[25] Approximately four layers of atoms at two ends were frozen as fixed walls to avoid atom evaporation, and approximately 18 layers of atoms were set to be cold and hot baths.

The LAMMPS (Large-scale Atomic/Molecular Massively Parallel Simulator) package was used in the NEMD simulations.[26] Accordingly, the Tersoff[27] potential was used to model the Si–Si, Ge–Ge, and Si–Ge atomic interactions. The NEMD-based method to compute the thermal conductivity is based on the momentum conservation scheme.[28] In the simulations, the MD time step is set to be 0.001 ps. First, the system was relaxed at zero pressure and a specific temperature in the NPT ensemble for 5000 ps. Following this, the optimized structure was obtained and the NVT was also performed for 1000 ps to make the system energy distribution state uniform at a desired temperature.

After system equilibration, a Langevin thermostat was used to generate a temperature gradient in the system, which was placed under NVE for 1000 ps to obtain the heat flux and calculate the thermal conductivity. The schematic diagram of the system that simulates the thermal transport across the Si/Ge interface is depicted in Fig. 2.

A typical averaged temperature profile obtained from the NEMD simulation is shown in Fig. 3, the temperatures of the hot and cold baths were maintained at 320 and 280 K, respectively, the temperature drop ΔT was estimated from the difference between the linear temperature profiles extrapolated to the interface as illustrated in Fig. 3.

The heat flux (J_x) was calculated using[29]

$$J_x = \frac{1}{A} \sum_{i \in \text{hot bath}} \frac{d}{dt} E_{i(t)}, \tag{1}$$

where E is the energy, t is the simulation time, and A is the cross-sectional area. The thermal conductivity κ is then calculated by using Fourier's law of heat conduction by[30,31]

$$\kappa = -\frac{J_x}{\left(\frac{\partial T}{\partial x}\right)}, \tag{2}$$

where J_x and $\partial T/\partial x$ are the heat flux and temperature gradient along the transport direction in the non-equilibrium steady state.

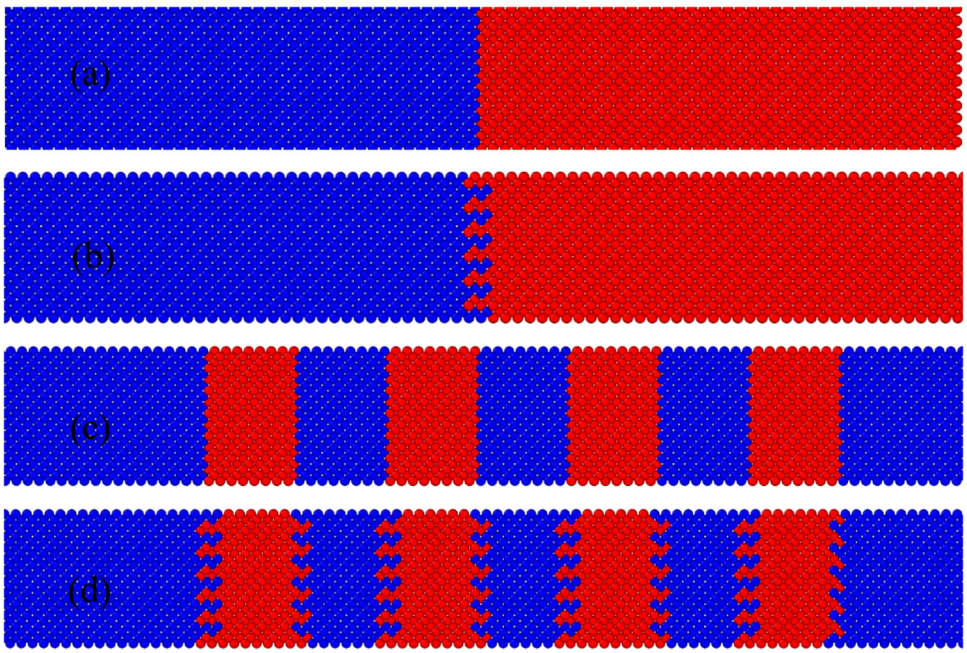

FIG. 1. Schematic of the structures simulated in this work and the corresponding atomic structure: (a) a single perfect interface; (b) a single atomic mixing interface; (c) a perfect multi-layer structure;(d) the multi-layer structure with n-layer atomic mixing interfaces.

To understand the underlying mechanisms of phonon transport, the phonon density of states (PDOS) has been studied. The PDOS is calculated from the Fourier transform of the velocity auto-correlation function[29,32]

$$\mathrm{PDOS}(\omega) = \frac{1}{\sqrt{2\pi}} \int e^{-i\omega t} \left\langle \sum_{j=1}^{N} v_j(t) v_j(0) \right\rangle, \tag{3}$$

where $v_j(0)$ is the average velocity vector of a particle j at initial time, $v_j(t)$ is its velocity at time t, and ω is the angular frequency.

The participation rate was calculated using lattice dynamics at 300 K. Mode localization can be quantitatively characterized by the participation ratio P_λ defined for each eigen-mode λ as

$$P_\lambda^{-1} = N \sum_i \left(\sum_\alpha \varepsilon_{i\alpha,\lambda}^* \varepsilon_{i\alpha,\lambda} \right)^2, \tag{4}$$

where N is the total number of atoms and $\varepsilon_{i\alpha,\lambda}$ is the αth eigenvector component of eigen-mode λ for the ith atom. The participation ratio can provide more detailed information about the localization effect for each mode.[33]

We also investigate the spectral heat flux by monitoring the force–velocity correlations across the interface, which is defined as[34,35]

$$q(\omega) = \frac{2}{A} Re \sum_{j \in Ge} \sum_{i \in Si} \int_{-\infty}^{\infty} d\tau e^{i\omega\tau} \langle F_{ij}(\tau) \cdot V_i(0) \rangle, \tag{5}$$

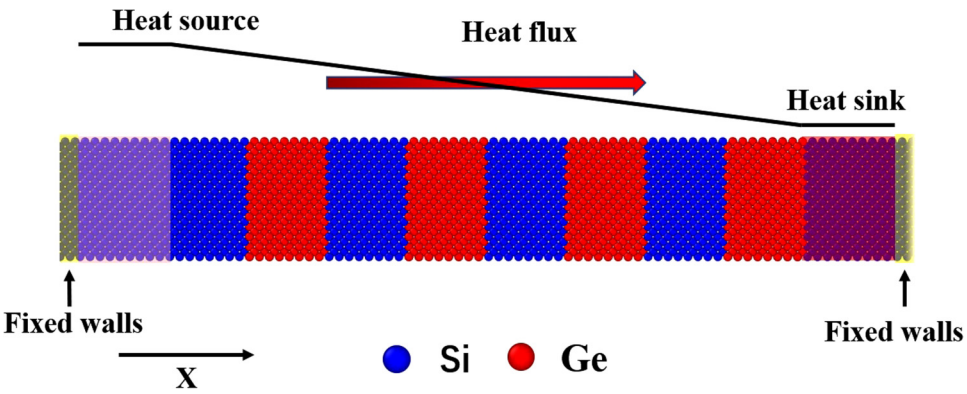

FIG. 2. Schematic diagram of the setup of the NEMD simulation.

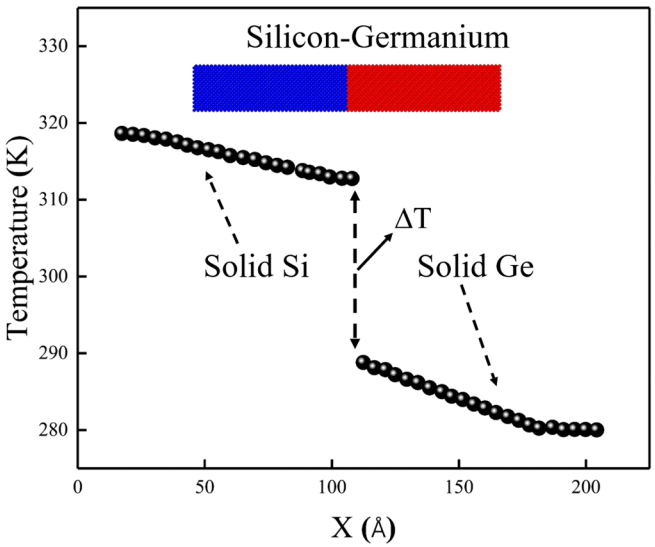

FIG. 3. Temperature profiles in the X direction of the simulated system for different atomic mixing layers at the Si/Ge interface at 300 K from NEMD.

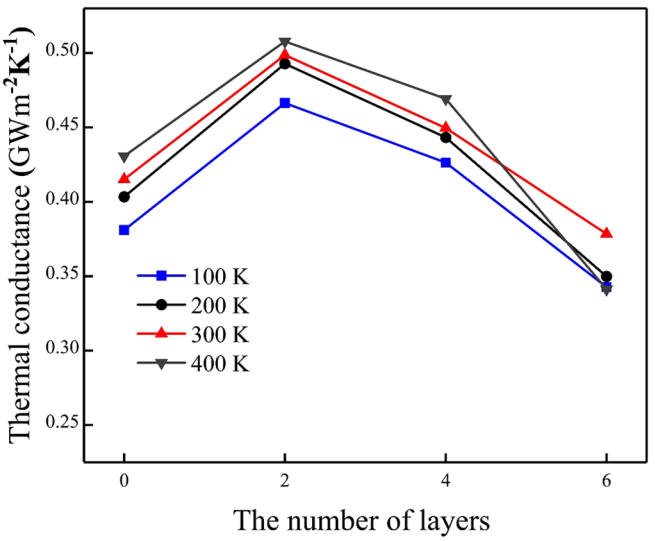

FIG. 4. Thermal conductance as a function of the number of atomic mixing layers at different temperatures.

where A is the interfacial area, V_i is the velocity of atoms on the interfacial Si sheet, F_{ij} is the force between Si and Ge atoms across the interface. The spectral interfacial thermal conductance $G(\omega) = |q(\omega)|/\Delta T$, ΔT is the temperature jump at the interface. And, the total interfacial thermal resistance can be calculated as[36]

$$\frac{1}{R} = \int_0^\infty \frac{d\omega}{2\pi} G(\omega) = \Delta f \frac{\sum_\omega |q(\omega)|}{\Delta T}, \tag{6}$$

where Δf is the discrete frequency interval.

III. RESULTS AND DISCUSSION

The thermal conductance for different models at a single Si/Ge interface was first calculated. To calculate the temperature profile along the X direction, the crystal is divided into several blocks as shown in Fig. 3. There is an obvious steep temperature drop ΔT between Si and Ge at the interface due to the thermal boundary resistance that is caused by an acoustic impedance mismatch, interfacial crystal defects, and other factors resulting in high interface phonon scattering. The value of the temperature drop is determined from the difference of the linear fits of the temperature profiles. The heat flux J_x across the Si/Ge interface is calculated using Eq. (1). The thermal conductance of the Si/Ge interface can be determined by $G = J_x/\Delta T$ from the combination of ΔT and J_x.

A. Effect of the interfacial atomic mixing on the thermal conductivity of the Si/Ge interface

The number of atomic mixing layers was varied, using 2, 4, and 6 layers to investigate the effects of the mixing layers on thermal transport across the Si/Ge interface. As shown in Fig. 4, the simulated results show that the thermal conductance of 2 and 4 mixing layers can be effectively improved under certain conditions compared with the perfect interface, which clearly indicates that it is possible to significantly improve the thermal transport across the Si/Ge interface by the atomic layer mixing at the interface. As the number of mixing layers increases, the thermal conductance increases first and then decreases; it reaches a maximum at two atomic mixing layers, which, at 300 K, is an increase of ~20% compared to the perfect interface, whereas for the four atomic mixing layers, it increased only by ~8% increase. To probe these mechanisms for the enhancement of the thermal conductance at the Si/Ge interface, the phonon density of states (PDOS) were calculated for the atoms in solid Si and solid Ge as well as atoms in different atomic mixing layers. The solid–solid thermal conduction is mainly affected by the overlap of the phonon spectrum of the two solids.[37] As shown in Fig. 5, the PDOS of solid Si and solid Ge are quite different, the PDOS of solid Si and solid Ge are mainly populated in frequencies between 5 and 17 THz, and between 2 and 12 THz, respectively.

Accordingly, a large difference in PDOS normally results in poor thermal transport across the interface.[5] The interfaces between Si and Ge with strongly contrasting Debye temperatures exhibit a very limited overlap between their corresponding phonon spectra.

Figure 5(a) shows the occupied PDOS for solid Si and solid Ge at 300 K. The small overlap between the two PDOS indicates that the thermal energy transport by elastic phonon scattering at the interface is very limited, which is responsible for the large interfacial thermal resistance of the perfect interface. As shown in Figs. 5(a) and 5(b), the Si/Ge mixture is introduced at the interface, which can serve as a bridge between solid Si and solid Ge, and the added overlap of phonon modes in PDOS provides additional volume for phonon frequency up or downconversion at the Si/Ge

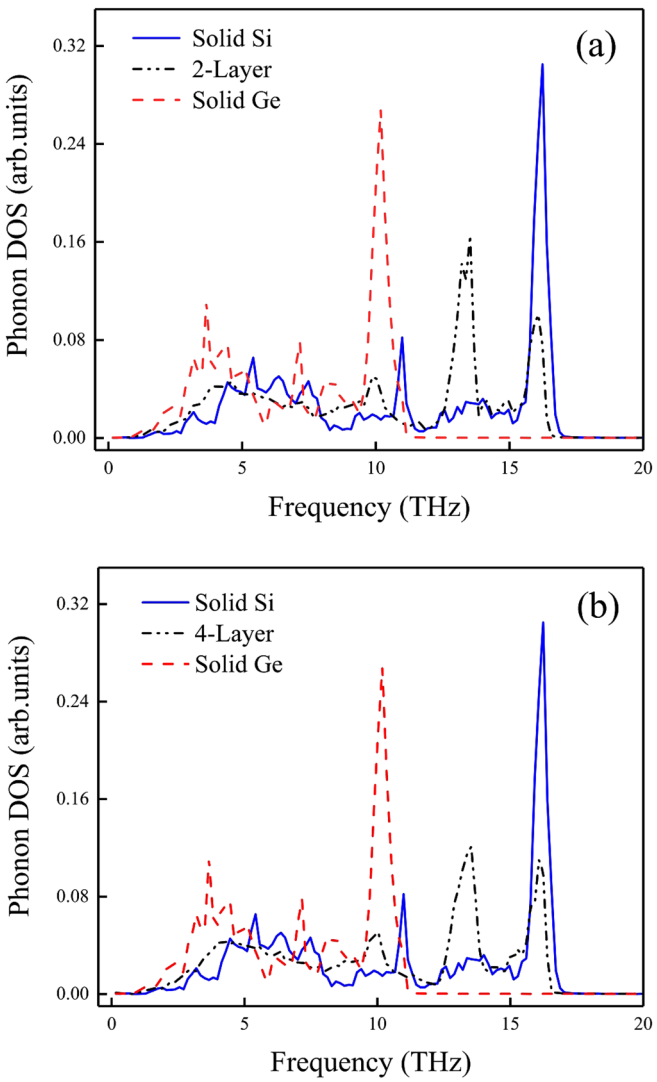

FIG. 5. PDOS as a function of frequency of different Si/Ge interfaces forms along the X direction at 300 K; (a) 2 atomic mixing layers; (b) 4 atomic mixing layers.

interface. The PDOS peaks of the 2-layer and 4-layer systems shift to a low frequency compared with that of solid Si, which indicates that the low-frequency phonons increased and the high-frequency phonons decreased. The low-frequency phonons have a greater possibility of phonon transmission at the interface, thus contributing to a larger thermal conductance at 2 and 4 mixing layers. However, as the number of atomic mixing layers increases, the thermal conductance does not continue to increase linearly. This is due to two competing factors: the overlapping PDOS increases the phonon transmission at the interface and the atomic mixing layers increase the diffuse scattering. These cause the highest thermal conductance of the two atomic mixing layers.

B. Effect of the interfacial atomic mixing on the thermal conductivity of multi-layer structures

Atomic mixing at the interface affects not only on the single interface but also the multi-interface structure of multi-layer structures. The thermal conductivities of these structures were computed as a function of the number of periods and period lengths. The thermal conductivities of the perfect interface and 2- and 4-layer interfacial atomic mixing multi-layer structures are shown in Fig. 6. Our previous study showed that the coherence length of phonon transport in the Si/Ge multi-layer structures was about ~4.34 nm,[38] therefore, in this study, the period length is set to 4.34 nm. As shown in Fig. 6, when the structures have fewer periods, interfacial atomic mixing enhances the thermal transport, though the enhancement is very limited. This indicates that interfacial atomic mixing can promote phonon transport of a single interface and a multi-layer structure with few periods due to a phonon "bridge" mechanism, which is consistent with the results in Sec. III A. In contrast, with an increasing number of periods, the thermal conductivity of the perfect MLS increases almost linearly, which is consistent with previous studies.[39,40] This suggests that phonon coherence transport, namely, the phonons coherently crossing the internal interfaces while maintaining the phase information, scatters only at the outermost interface, thus significantly affecting the thermal conductivity of the perfect interface. The thermal conductivities of the 2-layer and 4-layer atomic mixing multi-layer structures also increases, although the degree of increase is significantly lower than that of the perfect interface. This indicates that atomic mixing causes the destruction of coherent phonon transport. The lower increase in the thermal conductivity with the total length indicates that the atomic mixing does not entirely destroy all the phonon coherence

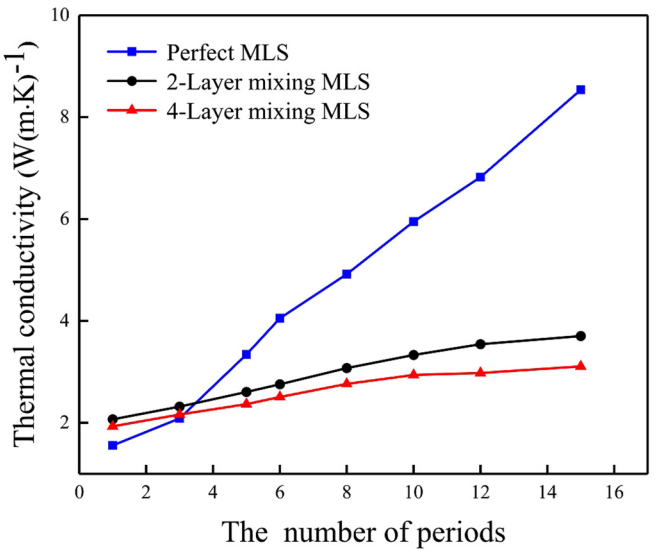

FIG. 6. Thermal conductivity of multi-layer structures as a function of number of periods for perfect and atomic mixing multi-layer structures at T = 300 K.

and a portion of the low-frequency phonons still undergo coherent transport.

In order to analyze the phonon transport properties in Fig. 6, the PDOS and the phonon participation ratio (PPR) of the 4-layer atomic mixing MLS and the perfect MLS were calculated while the total length was kept at 71.6 nm (15 periods). As shown in Fig. 7, the high-frequency PDOS peak of 4-layer atomic mixing MLS shifts to the lower frequencies compared with that of perfect MLS, this leads to a narrower frequency band of the mixing MLS, and its PDOS peak being lower than that of perfect MLS at high frequencies, both of which correspond to the lower thermal conductivity of the 4-layer atomic mixing MLS under certain conditions. To further study the phonon activities and their effects on the thermal transport, the PPR was calculated using Eq. (4). The participation ratio measures the fraction of atoms participating in a given mode and effectively indicates the localized modes with O (1/N) and delocalized modes with O (1). In thermal transport, delocalized modes mainly contribute to the thermal conductivity. Figure 8 compares the PPR of each eigen-mode of the perfect MLS and the 4-layer mixing MLS with 15 periods.

The value of the PPR in the 4-layer mixing MLS is significantly reduced for both low-frequency phonons and high-frequency phonons, compared with the perfect MLS. In our analyses, a PPR < 0.4 is taken as the criterion to ensure the localization of the most phonon modes. Compared with the perfect MLS, the majority of eigen-modes in the atomic mixing MLS has a participation ratio less than 0.4, which is characteristic of a localized mode. As a result, the thermal conductivity of the atomic mixing MLS is decreased compared with that of the perfect MLS. To further illustrate this, the spectral heat flux of the perfect MLS and 4-layer mixture MLS with 15 periods is shown in Fig. 9. The results show that the spectral heat flux of the perfect MLS is significantly higher than that of the 4-layer MLS. The high thermal conductivity of the perfect MLS is mainly due to the large contribution of low-frequency phonons to the heat transport, which indirectly indicates the strong coherent transport of phonons in the perfect MLS.

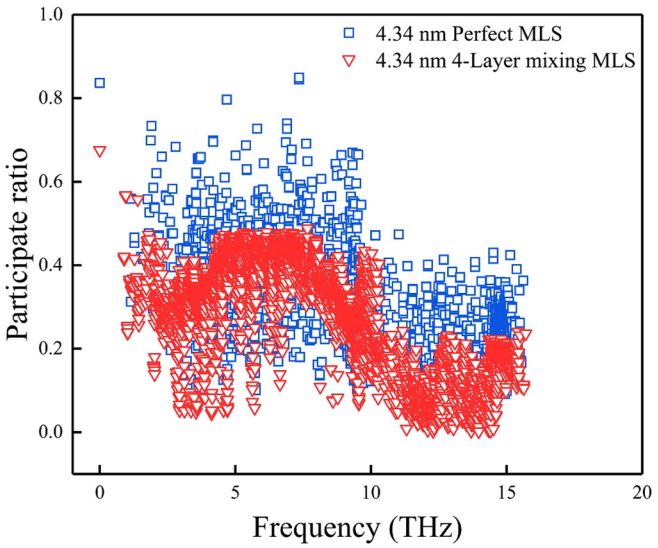

FIG. 8. Phonon participation ratio of perfect MLS and 4-Layer atomic mixing MLS with the total length of 71.6 nm.

We further studied the variation of the thermal conductivity of the multi-layer structures with different period lengths, as shown in Fig. 10. When the total length of the system is 71.6 nm, the thermal conductivity of the perfect MLS decreases first and then increases with the increase in the period length. The thermal

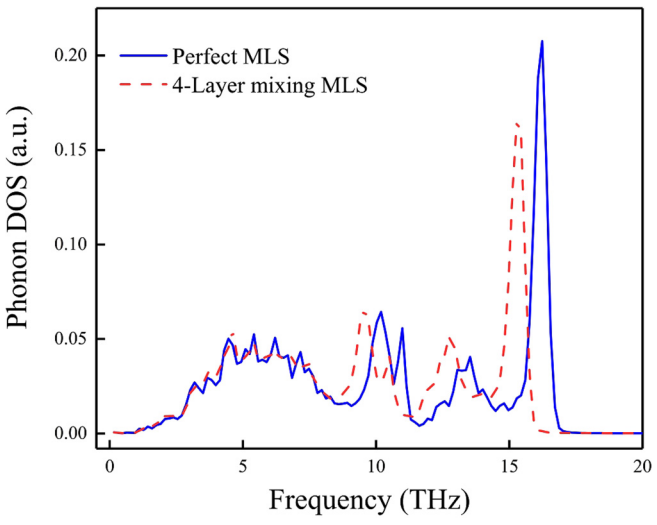

FIG. 7. Phonon DOS of perfect MLS and 4-layer atomic mixing MLS with the total length of 71.6 nm at 300 K.

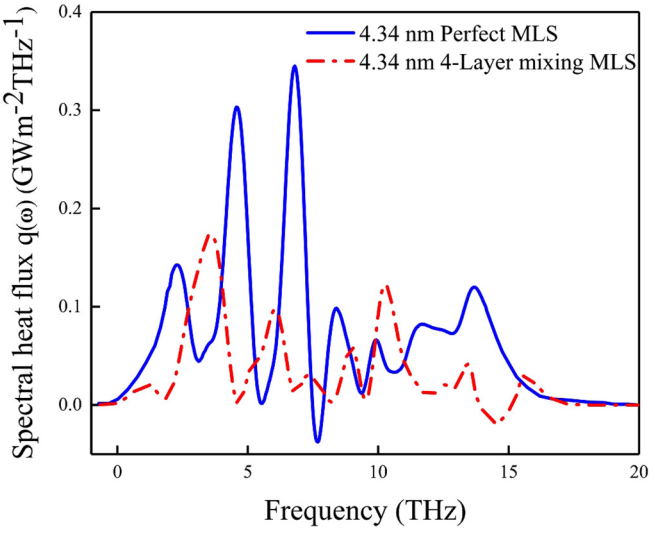

FIG. 9. Spectral thermal conductance across Si/Ge multi-layer structures at 300 K, the total length is kept at 71.6 nm and the period length is 4.34 nm.

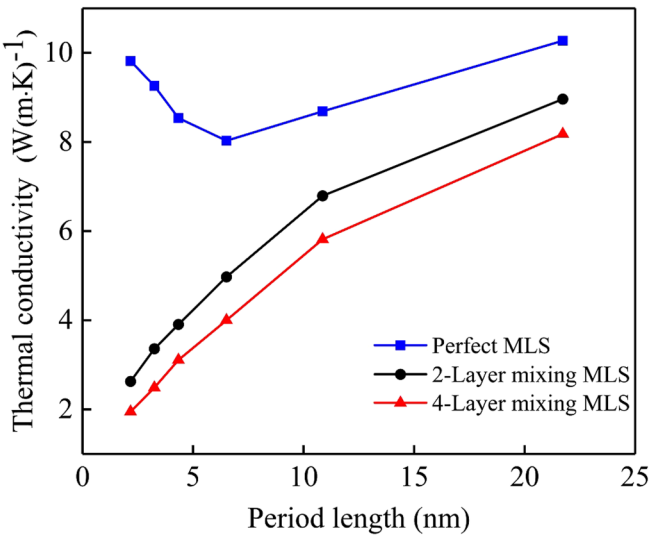

FIG. 10. Thermal conductivity of multi-layer structures as a function of period length at 300 K with the total length of 71.6 nm.

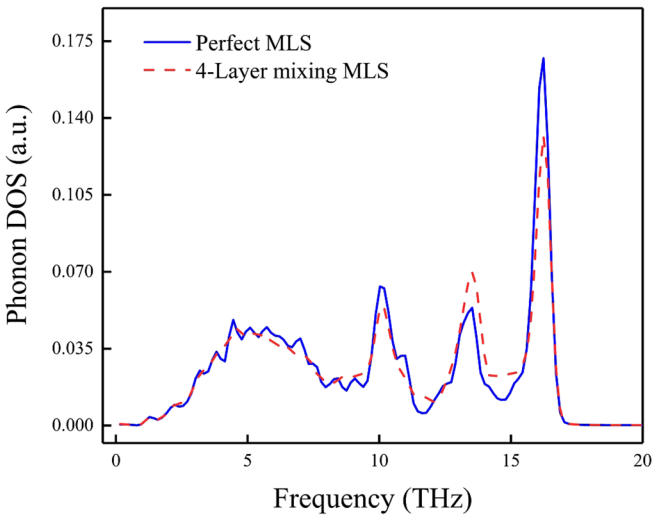

FIG. 11. PDOS of perfect MLS and the 4-layer atomic mixing MLS with a total length of 71.6 nm, a period length of 2.17 nm at 300 K.

conductivity decreases with the increase in the period length when the phonon is transported in the multi-layer structures, because the phonon's mean free path is equivalent to the period length and the phonon coherent transport is dominant. With the increase in the period length, the number of phonon microbands increases, which leads to a decrease in the phonon group velocity and, thus, the decrease in the thermal conductivity.[41,42] When the period length is further increased, the period length is larger than the mean free path of the phonons, and the incoherent diffusion transport becomes dominant. The decrease in the interface density reduces the phonon scattering at the interface, hence the thermal conductivity increases with the increase in the period length. The existence of a minimum value of thermal conductivity proves that the phonon transport is transformed from a wave coherent transport to a particle incoherent transport. However, unlike the perfect MLS, the thermal conductivity of the multi-layer structures with mixed atoms always increases with the increase of the period length. This indicates that atomic mixing at the interface destroys the majority of phonon coherence and phonon-interface scattering dominates the thermal transport, hence the thermal conductivity increases with the increase in the period length.

To explain the phenomenon in Fig. 10, the PDOS and PPR of the perfect MLS and the 4-layer mixing MLS were calculated at a period length of 2.17 nm at 300 K. As shown in Fig. 11, compared with the 4-layer mixing MLS, the PDOS of the perfect MLS has stronger peaks at high frequencies, which indicates that a greater number of phonon modes exist in the perfect MLS. Figure 12 compares the PPR of each eigen-mode for the perfect MLS and the 4-layer mixing MLS at a period length of 2.17 nm at 300 K, whereby a clear reduction of the PPR is observed in the 4-layer mixing MLS, both in the low- and high-frequency ranges.

We also compared the spectral heat flux of the perfect interface MLS and the 4-layer mixing MLS with a period length of 2.17 nm at 300 K, as shown in Fig. 13. The results show that in the perfect MLS, the heat flux of the high-frequency phonons of 10 THz is significantly higher than that of 4-layer MLS. The scattering of the high-frequency phonons is intense due to the atomic mixing at the interfaces.

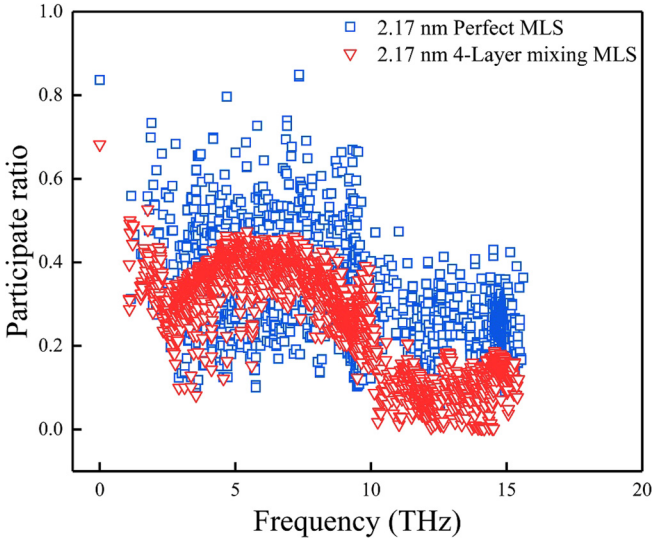

FIG. 12. Phonon participation ratio of the perfect MLS and the 4-layer atomic mixing MLS with a total length of 71.6 nm, a period length of 2.17 nm.

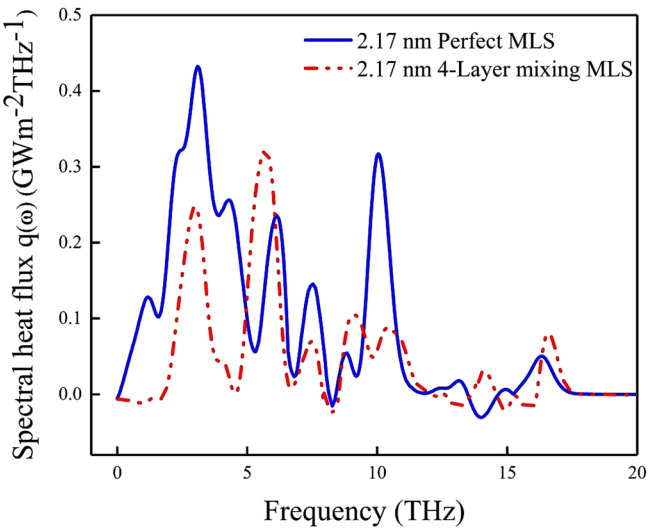

FIG. 13. Spectral thermal conductance across the Si/Ge multi-layer structures at 300 K. The total length and the period length are kept at 71.6 and 2.17 nm, respectively.

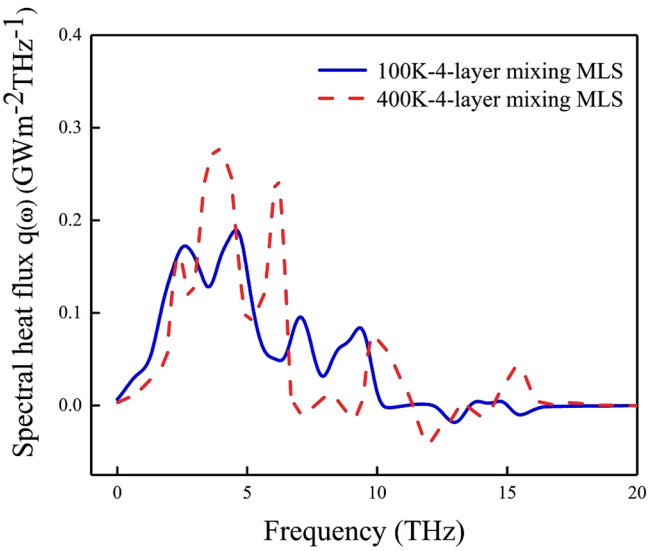

FIG. 15. Spectral thermal conductance of MLS with the 4-layer atomic mixture at 100 and 400 K. The number of periods is kept at 15, and the period length is kept at 4.34 nm.

Our simulations revealed the temperature dependence of perfect MLS and 4-layer mixing MLS. As shown in Fig. 14, thermal conductivities of perfect MLS and 4-layer mixing MLS show two different trends. For perfect MLS, as temperature increases, a fraction of coherent turns into incoherent phonons due to the lifetime of phonons decreases following $1/T$ trend,

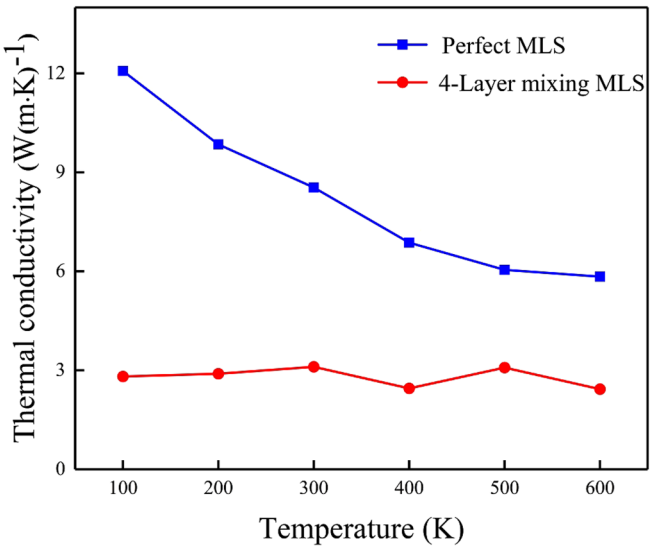

FIG. 14. Thermal conductivity variations of perfect MLS and 4-layer atomic mixing MLS. The number of periods is kept at 15.

which enhance the phonon–phonon Umklapp scattering. Thus, the thermal conductivity is decreased with increasing temperature, while the 4-layer mixing MLS are almost insensitive to the temperature. With the change of temperature, the change of thermal conductivity is not obvious. This may be related to the localization of phonons and phonon–phonon scattering. A large part of localized phonons in 4-layer mixing MLS is unable to deliver thermal energy. The deterioration of localized coherent phonons with increasing temperature enhances the thermal transport. While the increasing phonon–phonon scattering with increasing temperature decrease the thermal transport. The two competing factors cause almost weak increase in thermal conductivity. To further understand the underlying mechanism, as shown in Fig. 15, we compared the spectral heat flux of 4-layer mixing MLS at 100 and 400 K. The results show that in the range of 4–6 THz, the value of spectral heat flux at 400 K was significantly higher than that at 100 K, showing the enhancement of heat transport at this frequency range. However, in the range of 6–10 THz, the spectral heat flux of 400 K is lower than that of 100 K, indicating that the contribution of high-frequency phonons to heat transport is limited. Therefore, we attributed this temperature insensitivity to the localization of phonons and phonon–phonon scattering at 4-layer mixing MLS.

IV. CONCLUSION

In summary, the NEMD simulations were employed to investigate thermal transport in multi-layer structures with a single Si/Ge interface and mixture of Si/Ge at the interfaces. Both the 2-layer and 4-layer mixtures greatly enhanced the thermal transport across the interface; the maximum enhancement was achieved by the

2-layer Si/Ge mixture. A reduction of the interfacial thermal resistance was found, which was mainly due to the PDOS of the Si/Ge mixture, which bridges PDOS of the solid Si and solid Ge. For the Si/Ge multi-layer structures with fewer periods, the Si/Ge mixture at the interfaces could increase the thermal conductivity through a phonon "bridge" effect: as the number of periods increased beyond a certain number of periods, the thermal conductivity of the atomic mixing MLS would diminish significantly compared with the perfect MLS. This is most likely because the interface disorder destroys a large portion of the phonons' coherence, which could result in the transition from an incoherent to a coherent phonon dominated heat transfer regime.

The period length greatly affected the thermal conductivity. The thermal conductivity of perfect interfacial multi-layer structures showed a non-monotonic trend, which indicates that the phonon transport changed from the coherent transport of a wave to the diffusion transport of a particle. However, the interfacial atom mixing destroys the coherent phonon transport in the multi-layer structures, and the interfacial diffuse scattering plays a dominant role in phonon transport. Therefore, the thermal conductivity of the interfacial atom mixing multi-layer structures increased with the increase in the period length. Temperature can affect the thermal conductivity of the multi-layer structures in two ways. For the perfect MLS, as the temperature increases, the phonon–phonon scattering increases and the thermal conductivity decreases. For the atomic mixing MLS, the temperature insensitivity of the thermal conductivity may be attributed to the phonon localization and phonon–phonon scattering.

ACKNOWLEDGMENTS

The authors are grateful for funding from the National Natural Science Foundation of China (NNSFC) (No. 52076080), the Natural Science Foundation of Hebei Province (No. E2020502011), and the Fundamental Research Funds for the Central Universities (No. 2020MS105).

AUTHOR DECLARATIONS

Conflict of Interest

The authors have no conflicts to disclose.

DATA AVAILABILITY

The data that support the findings of this study are available from the corresponding author upon reasonable request.

REFERENCES

[1]D. G. Cahill, W. K. Ford, K. E. Goodson, G. D. Mahan, A. Majumdar, H. J. Maris, R. Merlin, and S. R. Phillpot, J. Appl. Phys. **93**, 793–818 (2003).
[2]Z. Li, S. Xiong, C. Sievers, Y. Hu, Z. Fan, N. Wei, H. Bao, S. Chen, D. Donadio, and T. Ala-Nissila, J. Chem. Phys. **151**, 234105 (2019).
[3]H. Zhao and J. B. Freund, J. Appl. Phys. **97**, 024903 (2005).
[4]Z. Zhang, Y. Ouyang, Y. Cheng, J. Chen, N. Li, and G. Zhang, Phys. Rep. **860**, 1–26 (2020).
[5]Z. Liang and H.-L. Tsai, J. Phys.: Condens. Matter **23**, 495303 (2011).
[6]W. Chen, J. Yang, Z. Wei, C. Liu, K. Bi, D. Xu, D. Li, and Y. Chen, Phys. Rev. B **92**, 134113 (2015).
[7]S. Merabia and K. Termentzidis, Phys. Rev. B **89**, 054309 (2014).
[8]Z. Liang and H.-L. Tsai, Int. J. Heat Mass Transfer **55**, 2999–3007 (2012).
[9]R. Hu, S. Iwamoto, L. Feng, S. Ju, S. Hu, M. Ohnishi, N. Nagai, K. Hirakawa, and J. Shiomi, Phys. Rev. X **10**, 021050 (2020).
[10]G. Chang, F. Sun, L. Wang, Z. Che, X. Wang, J. Wang, M. J. Kim, and H. Zhang, ACS Appl. Mater. Interfaces **11**, 26507–26517 (2019).
[11]M. R. Hasan, T. Q. Vo, and B. Kim, RSC Adv. **9**, 4948–4956 (2019).
[12]S. Jin, Z. Zhang, Y. Guo, J. Chen, M. Nomura, and S. Volz, Int. J. Heat Mass Transfer **182**, 122014 (2022).
[13]W. Ren, Y. Ouyang, P. Jiang, C. Yu, J. He, and J. Chen, Nano Lett. **21**, 2634–2641 (2021).
[14]P. J. O'Brien, S. Shenogin, J. Liu, P. K. Chow, D. Laurencin, P. H. Mutin, M. Yamaguchi, P. Keblinski, and G. Ramanath, Nat. Mater. **12**, 118–122 (2013).
[15]T. S. English, J. C. Duda, J. L. Smoyer, D. A. Jordan, P. M. Norris, and L. V. Zhigilei, Phys. Rev. B **85**, 035438 (2012).
[16]C. Shao and H. Bao, Int. J. Heat Mass Transfer **85**, 33–40 (2015).
[17]R. Rastgarkafshgarkolaei, J. Zhang, C. A. Polanco, N. Q. Le, and P. M. Norris, Nanoscale. **11**, 6254–6262 (2019).
[18]R. J. Stevens, L. V. Zhigilei, and P. M. Norris, Int. J. Heat Mass Transfer **50**, 3977–3989 (2007).
[19]B. Ni, T. Watanabe, and S. R. Phillpot, J. Phys.: Condens. Matter **21**, 084219 (2009).
[20]Z. Tian, K. Esfarjani, and G. Chen, Phys. Rev. B **86**, 235304 (2012).
[21]L. Jia, S. Ju, X. Liang, and X. Zhang, Mater. Res. Express **3**, 095024 (2016).
[22]J. Ravichandran, A. K. Yadav, R. Cheaito, P. B. Rossen, A. Soukiassian, S. J. Suresha, J. C. Duda, B. M. Foley, C. H. Lee, Y. Zhu, A. W. Lichtenberger, J. E. Moore, D. A. Muller, D. G. Schlom, P. E. Hopkins, A. Majumdar, R. Ramesh, and M. A. Zurbuchen, Nat. Mater. **13**, 168–172 (2014).
[23]M. N. Luckyanova, J. Mendoza, H. Lu, B. Song, S. Huang, J. Zhou, M. Li, Y. Dong, H. Zhou, J. Garlow, L. Wu, B. J. Kirby, A. J. Grutter, A. A. Puretzky, Y. Zhu, M. S. Dresselhaus, A. Gossard, and G. Chen, Sci. Adv. **4**, eaat9460 (2018).
[24]P. Chakraborty, L. Cao, and Y. Wang, Sci. Rep. **7**, 8134 (2017).
[25]P. K. Schelling, S. R. Phillpot, and P. Keblinski, Phys. Rev. B **65**, 144306 (2002).
[26]S. Plimpton, J. Comput. Phys. **117**, 1–19 (1995).
[27]Y. He, D. Donadio, and G. Galli, Appl. Phys. Lett. **98**, 144101 (2011).
[28]Z. Huang and Z. Tang, Phys. B: Condens. Matter **373**, 291–296 (2006).
[29]X. Qu and J. Gu, RSC Adv. **10**, 1243–1248 (2020).
[30]Y. Liu, Y. Bian, A. Chernatynskiy, and Z. Han, Int. J. Heat Mass Transfer **145**, 118791 (2019).
[31]C. Choi and N. Roberts, Int. J. Therm. Sci. **104**, 13–19 (2016).
[32]V. Samvedi and V. Tomar, Nanotechnology **20**, 365701 (2009).
[33]J. Chen, G. Zhang, and B. Li, Nano Lett. **10**, 3978–3983 (2010).
[34]K. Sääskilahti, J. Oksanen, J. Tulkki, and S. Volz, Phys. Rev. B **90**, 134312 (2014).
[35]Y. Sun, Y. Zhou, J. Han, M. Hu, B. Xu, and W. Liu, J. Appl. Phys. **127**, 045106 (2020).
[36]Y. Ma, Z. Zhang, J. Chen, K. Sääskilahti, S. Volz, and J. Chen, Carbon **135**, 263–269 (2018).
[37]M. Hu and D. Poulikakos, Int. J. Heat Mass Transfer **62**, 205–213 (2013).
[38]Y. Liu, J. Hao, G. Ren, and J. Zhang, Acta Phys. Sin. **70**, 84 (2021).
[39]Y. Wang, C. Gu, and X. Ruan, Appl. Phys. Lett. **106**, 073104 (2015).
[40]Z. Tian, K. Esfarjani, and G. Chen, Phys. Rev. B **89**, 235307 (2014).
[41]K. Termentzidis, S. Merabia, P. Chantrenne, and P. Keblinski, Int. J. Heat Mass Transfer **54**, 2014–2020 (2011).
[42]E. S. Landry and A. J. H. McGaughey, Phys. Rev. B **79**, 075306 (2009).